Advances in EKF SOC Estimation for LiPB HEV Battery Packs

Gregory L. Plett
University of Colorado at Colorado Springs and consultant to Compact Power Inc.

Abstract

This paper describes advances in models and methods used to estimate hybrid-electric-vehicle (HEV) battery-pack state-of-charge (SOC) using extended Kalman filtering (EKF). The electrochemical cells in the battery pack are Lithium Ion Polymer based, have a nominal capacity of about 7.5 Ah, and are optimized for power-needy applications. The discharge curve of these cells is very flat, which is desirable for some reasons, but also makes SOC estimation quite challenging and motivates the use of advanced methods.

In earlier papers [1–2], we presented several cell models that may be used with the EKF method, and the EKF method of SOC estimation itself. Our best cell model was a "Radial Basis Function" (RBF) type, whose parameters were optimized by a "black-box" system identification procedure. We have subsequently found that although this model worked well on a cell level, it was too slow and exhibited unreliable performance when ported to the battery management system of the pack.

In this paper, we describe a new cell model that alleviates these problems. The model parameters are optimized by "gray-box" system identification and most have direct physical interpretation. The model structure includes effects of: internal resistance, hysteresis, and relaxation time constants. It is greatly simplified with respect to the RBF model, allowing the SOC estimation algorithm to execute in about 1/50 of the time it did before.

Results indicate that the new cell model with EKF provides SOC estimates that are about as precise as those made with RBF, but are more accurate and reliable.

Keywords: Battery model, battery management, lithium polymer, state of charge, HEV.

1. Introduction

This paper describes advances in models and methods used to estimate hybrid-electric-vehicle (HEV) battery-pack state-of-charge (SOC) using extended Kalman filtering (EKF). The electrochemical cells in the battery pack are Lithium Ion Polymer based, jointly developed by LG Chem Ltd. (Daejeon, Korea) and Compact Power Inc. (Colorado, USA), have a nominal capacity of about 7.5 Ah, and are optimized for power-needy applications. The discharge curve of these cells is very flat, which is desirable for some reasons, but also makes SOC estimation quite challenging and motivates the use of advanced methods. The EKF method, in particular, is able to achieve very good results [2], and provides the additional feature of supplying dynamic error bounds on the SOC estimate.

In order to use EKF to estimate SOC, we require an electrical input-output model of the behavior of Lithium Ion Polymer Battery (LiPB) cells. The cells are treated as nonlinear dynamic systems, represented in a discrete-time state-space form. Specifically, we assume the form

$$x_{k+1} = f(x_k, u_k) + w_k \quad (1)$$

$$y_k = g(x_k, u_k) + v_k, \quad (2)$$

where x_k is the system state vector at discrete-time index k, u_k is the measured exogenous system input at time k (which may include measurements of battery-pack current, temperature and so forth) and w_k is unmeasured "process noise" affecting the system state (and also models the inaccuracy of the cell model,

to some extent). The system output is y_k, and v_k is the measurement noise that usually models noise in sensors. Equation (1) is called the "state equation", (2) is called the "output equation", and $f(\,)$ and $g(\,)$ are (possibly nonlinear) functions, specified by the particular cell model used.

To be more specific, the system input vector u_k typically contains the instantaneous cell current i_k. It may also contain the cell temperature T_k, an estimate of the cell's capacity C, and/or an estimate of the cell's internal resistance R_k, for example. The system output is typically a scalar but may be vector valued as well. Here we consider the output to be the cell's loaded terminal voltage—not at-rest open-circuit-voltage (OCV). The system's state vector x_k in some way represents in summary form the total effect of all past input to the system so that the present output may be predicted solely as a function of the state and present input. Values of past inputs are not required. Our method constrains the state vector to include SOC as one component, so that SOC may later be estimated using EKF.

Many cell models have been proposed in the literature for many purposes. References [1,3] outline a number of these. The specific application we have in mind is to model cell dynamics for the purpose of state-of-charge estimation in a hybrid electric vehicle (HEV) battery pack. The HEV application is a very harsh environment with rate requirements up to about ±25C, very dynamic rate profiles, and operating temperatures between –30ºC and 50ºC. This is in contrast to relatively benign portable-electronic applications with constant power output and fractional C rates. Methods for cell modeling and SOC estimation that work well in portable electronic devices often fail in the HEV application. If precise SOC estimation is required by the HEV, then a very accurate cell model is necessary.

In earlier papers [1–2], we presented several cell models that may be used with the EKF method, and the EKF method of SOC estimation itself. Our best cell model was a "Radial Basis Function" (RBF), whose parameters were optimized by a "black-box" system identification procedure. We have subsequently found that although this model worked well on the cell level, it was too slow and exhibited unreliable performance when implemented in the battery management system of a pack. In this paper, we describe a new cell model that alleviates these problems. The model parameters are optimized by "gray-box" system identification and most of the parameters have direct physical interpretation. The model structure includes effects of: internal resistance, hysteresis, and relaxation time constants. The model parameters vary with temperature to give good SOC estimation over a wide range of operating conditions. It is also greatly simplified with respect to the RBF model, allowing the SOC estimation algorithm to execute in about 1/50 of the time it did before. The method is also very general, and we expect it to work well in many other battery systems with different chemistries and applications.

This paper is organized as follows: First, we review cell models from [1], and explain their shortcomings. Secondly, we present some evolutionary changes to these models that have improved performance, along with methods for determining model parameters. The testing equipment, cells and regimen for cell modeling are described. Finally, the results are evaluated and conclusions made.

2. Legacy Cell Models

In order to use the Kalman methods we propose to estimate SOC, the cell model must be represented in the discrete-time state-space form of (1) and (2) (with the constraint that SOC is a member of the state vector). The difference between the models, then, depends only on the definitions of x_k, u_k, $f(\,)$ and $g(\,)$.

The basis for the SOC state-equation is developed as follows: If $z(t) = \text{SOC}$, we know that

$$z(t) = z(0) - \int_0^t \frac{\eta(i(\tau))\, i(\tau)}{C}\, d\tau, \tag{3}$$

where C is the nominal capacity of the cell, $i(t)$ is the cell current at time t, and $\eta(i(t))$ is the Coulombic efficiency of the cell. A discrete-time approximate recurrence may then be written as

$$z_{k+1} = z_k - \frac{\eta(i_k)\, i_k\, \Delta t}{C}, \tag{4}$$

where Δt is the sampling period (in hours). Equation (4) is used to include SOC in the state vector of the cell model as it is in state equation format already, with SOC as the state and i_k as the input. Our cell models will then be differentiated by the additional components in the state vector and the functional form of $f(\,)$ and $g(\,)$.

2.1 The Single-State "Combined" Cell Model

The simplest models in [1] have a single state—SOC—and so share a common state equation (4). The difference between them is the output equation. Several different forms were suggested, culminating in the "combined" cell model that includes all of the terms from the individual forms:

$$y_k = \underbrace{K_0 - K_1 / z_k - K_2 z_k + K_3 \ln(z_k) + K_4 \ln(1 - z_k)}_{fn(z_k)} - \underbrace{R i_k}_{fn(i_k)}, \tag{5}$$

where y_k is the cell terminal voltage, R is the cell internal resistance (different values may be used for charge/discharge and at different SOC levels if desired), and K_0 through K_4 are constants chosen to make the model fit the data well. The unknown quantities in (5) may be estimated using a system identification procedure from cell test data.

2.2 The Four-State "Filter-State" Cell Model

The combined model of (5) may be very quickly identified and implemented. Its serious limitation is that it omits any description of cell voltage relaxation during rest periods (and equivalently, time constants on dis/charge events). Since the cell model must accurately predict true cell behavior in a dynamic HEV environment, we find it is essential to include these relaxation effects.

The filter-state model adds states to explain relaxation effects: a single-state filtered SOC, and two-state filtered input current. The state that filtered SOC was implemented as:

$$f_k^z = w_1 z_{k-1} + w_2 f_{k-1}^z + w_3. \tag{6}$$

The states that filtered i_k were implemented as:

$$\begin{bmatrix} f_k^I \end{bmatrix} = \begin{bmatrix} w_4 & w_5 \\ -w_5 & w_4 \end{bmatrix} \begin{bmatrix} f_{k-1}^I \end{bmatrix} + \begin{bmatrix} 0 \\ 1 \end{bmatrix} I_k^{\text{mod}}. \tag{7}$$

The output equation may be written as:

$$y_k = \underbrace{w_6 + \frac{w_8}{z_k + w_9} + w_{10} z_k + 10 f_k^z}_{fn(z_k)} + \underbrace{\begin{bmatrix} w_{11} & w_{12} \end{bmatrix} \begin{bmatrix} f_k^I \end{bmatrix} + w_7 I_k^{\text{mod}}}_{fn(I_k)}. \tag{8}$$

where $I_k^{\text{mod}} = \eta(i_k)\, |i_k|^n \Delta t / C_p$, n is the Peukert exponent and C_p is the Peukert capacity. The output y_k is terminal voltage, as before. The parameters of the model may be found by system identification using measured cell data. We found that the model was able to predict cell behavior best when different sets of parameters were used for different levels of input current i_k.

2.3 The Fully Nonlinear "Radial Basis Function" (RBF) Cell Model

Adding linear filter states to the model did improve its ability to predict a cell's behavior. However, as

the LiPB cells themselves are nonlinear systems, we felt that we could improve even further by considering a fully nonlinear dynamic cell model. For this purpose, we used radial-basis-function (RBF) networks and a black-box system identification procedure.

An RBF network makes a local approximation of the function it models. It computes its output as a weighted sum of (hyper) Gaussian shapes. Specifically, it computes the function

$$y_k = \sum_{j=1}^{N} w_j \exp\left(-\frac{1}{\sigma_j^2} \left\| u_k - t_j \right\|^2 \right) + w_{N+1}, \tag{9}$$

where N is the number of bases, w_j is the weight connecting the jth basis function to the output, σ_j is the "standard deviation" or width parameter of the jth basis function, x_k is the vector input to the network, and t_j is the center of the jth basis function. The parameters w_k of the RBF network may be identified from data using a system-identification procedure. Here, u_k includes the states of the system: *e.g.,* $x_k = [y_{k-1}, \mathrm{SOC}_k]^T$ as well as the cell current i_k.

2.4 Problems with the Legacy Cell Models

Subsequent to papers [1–2], we implemented the RBF model, along with its EKF SOC estimator, in a 40-cell battery management system. We chose RBF because of its seemingly superior attributes: very precise cell modeling, scalable complexity (accuracy could be improved to any desired level by adding more basis function kernels), and very accurate SOC prediction and fast recovery in the event of a bad initial SOC guess.

However, many of these attributes, validated in simulation, did not result in anticipated performance in the actual implementation. Some simple tests showed a lack of robustness:

1) A constant-current charge/discharge should make the SOC ramp up/down at the slope *I/C* [A/Ah]. In practice, the slope using RBF was often wrong.
2) During a rest period, cell terminal voltage converges to OCV (neglecting hysteresis effects, described later), and estimated SOC should converge to the SOC predicted by OCV. In the implementation, we observed SOC to drift considerably, not converging to the correct value.

Why? The most convincing explanation of the RBF model's failure is based on a vulnerability of all non-linear models. These models will predict system behavior best when the system is operating in the same regime where data was collected to train the model. If the system is operating in some other regime, the model must interpolate or extrapolate its learned behavior (a phenomenon known as *generalization*). While RBF systems are known to generalize "well", this one was not able to generalize enough. The learned behavior was a sequence of HEV drive cycles, which were too different from constant current or rest to be able to extrapolate model behavior.

This paper proceeds to discuss some insights into the three cell models, garnered from hindsight, and uses them to craft a new cell model. In particular, the new model forces y_k to converge to OCV after a rest period, and it forces y_k to converge to OCV–I×R for a constant-current dis/charge. Furthermore, the cell model is much simpler than RBF, allowing much faster execution of the SOC algorithm.

3. Evolutionary Changes to Improve the Cell Models

3.1 Discussion of the Legacy Cell Models

Discussion of the Combined Model

The combined-model output equation is a static function of SOC and cell current i_k. It may be broken into two additive parts: a part depending only on SOC, and another depending only on i_k, as shown in (5).

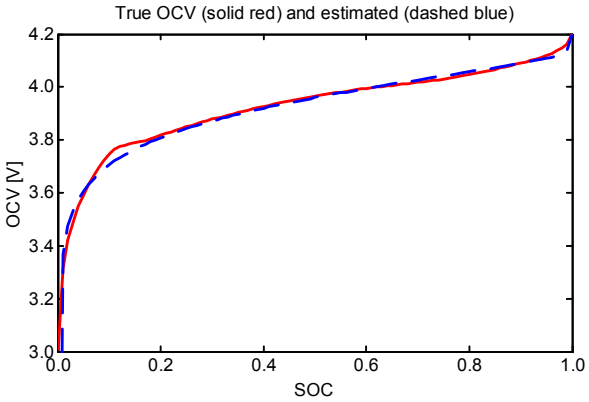

Figure 1: True OCV and OCV estimated by "combined" model, plotted versus SOC.

The part depending only on SOC bears closer examination. When parameter values $\{K_0 \ldots K_4\}$ are fit to this function, we plot it versus SOC and get the result in Figure 1 (dashed blue curve). Overlaid is the OCV as a function of SOC (solid red curve). We see that this function is trying to fit OCV(z_k). So, a better model—using table-lookup (for example) for OCV as a function of SOC—is:

Simple model: $y_k = \text{OCV}(z_k) - R\, i_k.$ (10)

An examination of [1, Fig. 2], reproduced as Figure 2 here,[1] shows that the combined model predicted y_k well when a constant charge/discharge cycle was taking place, but the rest voltage was incorrect. This is partially explained by the difference between the two curves in Figure 1 and partially by cell hysteresis (note that the cell voltage is always lower than model voltage on discharge, and greater on charge). Using (10), we get the results in Figure 3, which are very similar to those of Figure 2, but are accomplished with a simpler model. Cell relaxation effects are still ignored.

Discussion of the Filter State Model

Examining the filter-state model output equation in (8), we see that the output again breaks up into a function of SOC plus a function of i_k. Hindsight shows that the function of SOC was a poor choice. There is no guarantee that $y_k \to \text{OCV}$ in a rest period, the OCV characteristic is not modeled well as a function of SOC, and further work indicates that filter states on SOC are not necessary. The function of i_k also does not guarantee that $y_k \to \text{OCV(SOC)} - I \times R$ on constant-current dis/charge.

Discussion of the RBF Model

The output of the RBF model in (9) is not separable into additive parts based on SOC and on i_k. RBF is very much a black-box approach to cell modeling and gives no insight into cell behavior. In addition, no guarantee is given that $y_k \to \text{OCV}$ in a rest period or $y_k \to \text{OCV(SOC)} - I \times R$ on CC dis/charge.

3.2 The Self-Correcting Model

Based on experience gained from the preceding, it appears that a cell model needs to be of the form:

$$y_k = \underbrace{\text{OCV}(z_k)}_{fn(z_k)} + \underbrace{\text{filt}(i_k) - i_k R}_{fn(i_k)}. \quad (11)$$

[1] The cell tests performed for Figures 2–5 are discussed in greater detail in Section 4. Here, our goal is for the cell-model predicted voltage to closely approximate the true cell voltage.

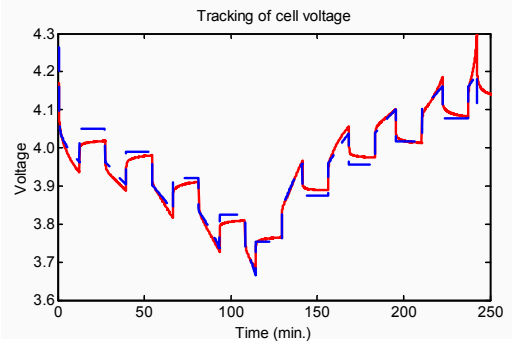

Pulsed current at ±1C rates.

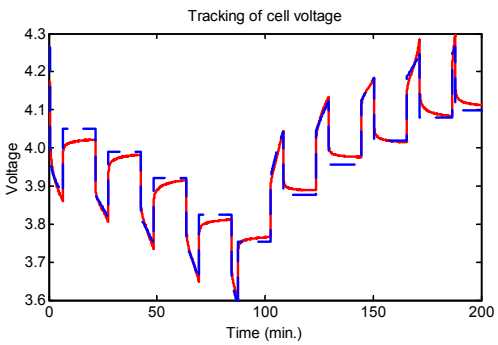

Pulsed current at ±2C rates.

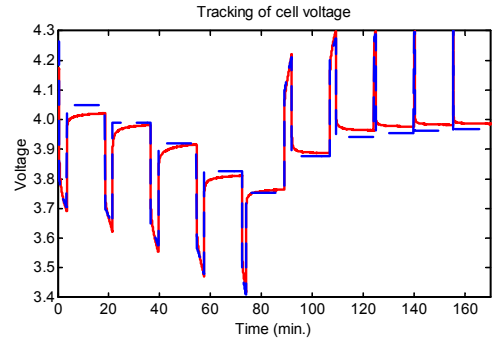

Pulsed current at ±4C rates.

Figure 2: Cell voltage tracking using the "combined" model from [1]. Solid red line is true cell voltage; dashed blue line is voltage predicted by cell model. Cell tests were pulsed current at ±1C, ±2C and ±4C rates, punctuated with rest periods.

This is again separable into a part based on SOC and another based on i_k. SOC contributes the long-term dc level (bias) to the output and i_k and its history contribute the short-term variation around this level. SOC is no longer filtered, as in the filter-state version and RBF versions—it does not make sense to have a moving bias point.

The filter "filt( )" must satisfy two criteria: (1) After a long rest period its output must be zero so that $y_k \to \text{OCV}$; (2) During a constant-current dis/charge, its output must converge to zero so that $y_k \to \text{OCV(SOC)} - I \times R$. The first criterion is satisfied by a stable linear filter, and the second is satisfied by a linear filter with zero dc gain. Both of these may be enforced in the filter design.

The self-correcting model is:

$$\left[f_k^I\right] = \left[\text{diag}(\alpha)\right]\left[f_{k-1}^I\right] + i_k \tag{12}$$

$$y_k = \text{OCV}(z_k) + C\left[f_k^I\right] - Ri_k . \tag{13}$$

The vector α has N filter "poles" with $|\alpha| < 1$, and C has N weighting parameters. There are $2N+2$ parameters to the model, assuming that both charge and discharge resistances are modeled, and a value of $N \approx 4$ works well. This is much fewer than the 900^+ parameters for the RBF model.

We compare Figure 4 with [1, Figs. 2–4]. The prediction of the self-correcting model appears to be on par with the filter state model in [1, Fig. 3], but somewhat worse than the RBF model in [1, Fig. 4].

Results of EKF SOC estimation using the self-correcting model are better than the SOC prediction of the "combined" model, and a little worse than the SOC prediction of the RBF model. However, the model is much more robust due to its self-correcting nature. In particular, when the initial SOC guess is incorrect, the self-correcting model very quickly recovers the correct SOC. It is on the same order of speed as the

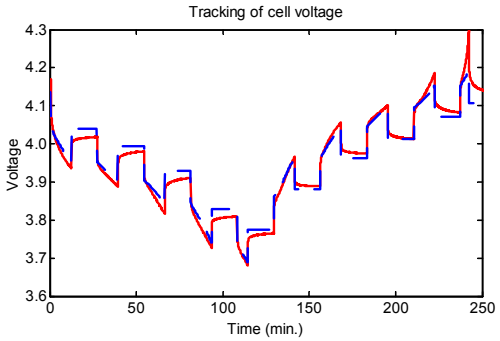

Pulsed current at ±1C rates.

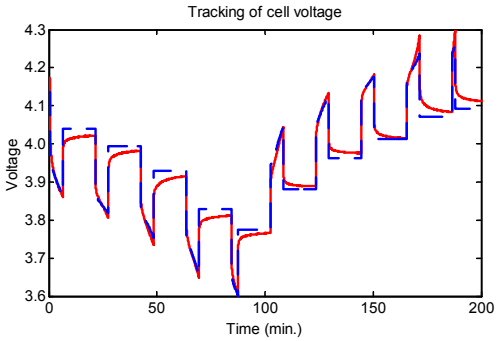

Pulsed current at ±2C rates.

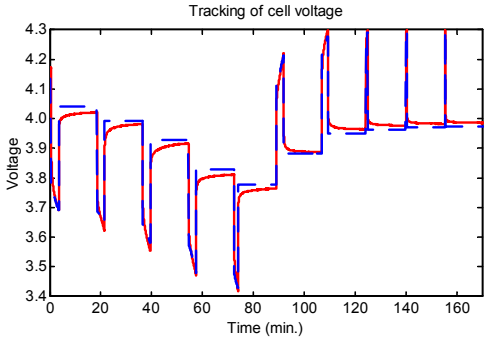

Pulsed current at ±4C rates.

Figure 3: Cell voltage tracking using the "simple" model of (10). Solid red line is true cell voltage; dashed blue line is voltage predicted by cell model. Cell tests were pulsed current at ±1C, ±2C and ±4C rates, punctuated with rest periods.

"combined" model, and much better than the other two models. This may be explained by noticing that the voltage bias is dependent only on SOC, not filtered versions thereof, nor mixtures of SOC and i_k. In the "credit assignment problem" that assigns credit/blame for the difference between the measured voltage and estimated voltage, the Kalman filter can now blame a bad bias point on the SOC state and poor dynamic fluctuation on the filter states. This was the downfall of the filter-state model where SOC provided a moving bias point, and a constant bias modeling error might then be attributed to both SOC states and filter states, diluting the true blame.

3.3. The Enhanced Self-Correcting Model

The self-correcting model structure worked quite well in an actual implementation, so long as the pack was at room temperature. Performance at low temperatures was poor.[2] We have found that cell voltage hysteresis is considerable at low temperature and must be included in the model. (For a good paper describing electrochemical hysteresis, see Reference [4]).

The term hysteresis is derived from the Greek *hustereia*, "to arrive late". The cell voltage lags the predicted voltage in some sense. A more appropriate definition for us might be "a characteristic of a system in which a change in the direction of the independent variable (cell current) leads to the dependent variable (cell voltage) failing to retrace the path it followed in the forward direction." [4] The bottom line is that for each SOC there are more than one stable at-rest cell voltages (a range of values are possible).

We illustrate this by showing dis/charge curves at the C/25 rate at 20ºC in Figure 6. The terminal voltage for discharge is the lower curve, and the terminal voltage for charge is the upper curve. Two distinct

[2] Full temperature-dependent cell modeling is beyond the scope of the discussion here.

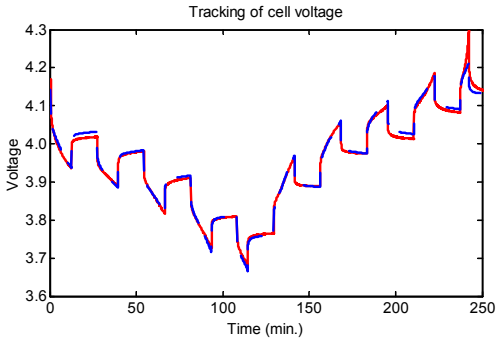

Pulsed current at ±1C rates.

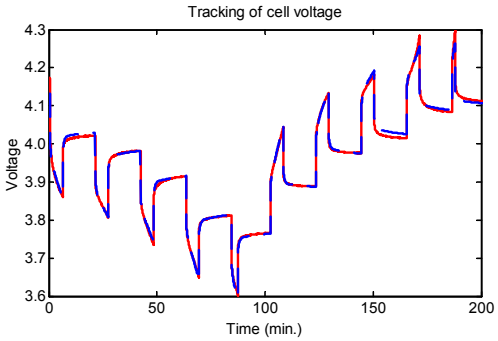

Pulsed current at ±2C rates.

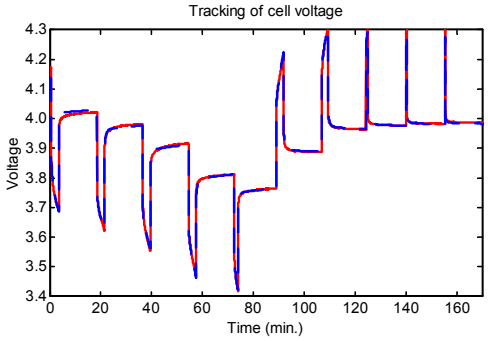

Pulsed current at ±4C rates.

Figure 4: Cell voltage tracking using the self-correcting model of (12)–(13). Solid red line is true cell voltage; dashed blue line is voltage predicted by cell model. Cell tests were pulsed current at ±1C, ±2C and ±4C rates, punctuated with rest periods.

voltages exist for each SOC. Half the difference between these voltages is the polarization voltage of the cell. Only a small part of the polarization is due to the $I \times R$ drop (about 1.2mV here) and the remainder is due to hysteresis effects (about 25mV here).

These curves comprise the "major hysteresis loop," corresponding to full cell charge and discharge. Minor hystereses loops are encountered when a partial charge is followed by a partial discharge, and vice versa. The polarization does not immediately flip sign on a current reversal but slowly decays from one leg of the major hysteresis loop to the other. This transition may be modeled by adding a "hysteresis state" to the state equation. The hysteresis state is not a differential equation in time but in SOC. Let $h(t)$ be the hysteresis voltage as a function of time, and let $\dot{z} = dz/dt$. Then,

$$\frac{dh(z,t)}{dz} = \gamma \, \mathrm{sgn}(\dot{z})\big(M(z,\dot{z}) - h(z,t)\big), \tag{14}$$

where $M(z,\dot{z})$ is a function that gives the maximum polarization due to hysteresis as a function of SOC and the rate-of-change of SOC. Specifically, $M(z,\dot{z})$ is positive for charge ($\dot{z} > 0$) and is negative for discharge ($\dot{z} < 0$). The $M(z,\dot{z}) - h(z,t)$ term in the differential equation states that the rate-of-change of hysteresis voltage is proportional to the distance away from the major hysteresis loop, leading to a kind of exponential decay of voltage to the major loop. The term in front of this has a positive constant γ, which tunes the rate of decay, and $\mathrm{sgn}(\dot{z})$, which forces the equation to be stable for both charge and discharge.

In order to fit the differential equation for $h(z,t)$ into our model, we must manipulate it to be a differential equation in time, not in SOC. We accomplish this by multiplying both sides of the equation by dz/dt.

$$\frac{dh(z,t)}{dz}\frac{dz}{dt} = \gamma \, \mathrm{sgn}(\dot{z})\big(M(z,\dot{z}) - h(z,t)\big)\frac{dz}{dt}. \tag{15}$$

Note that $dz/dt = -\eta(i(t))i(t)/C$, and that $\dot{z}\,\mathrm{sgn}(\dot{z}) = |\dot{z}|$. Thus,

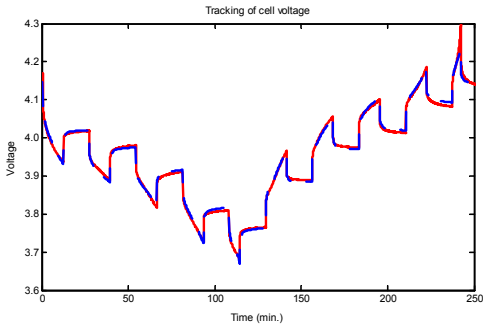

Pulsed current at ±1C rates.

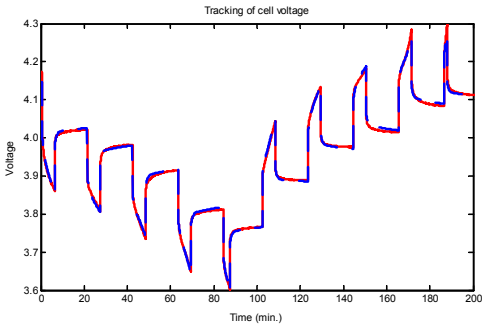

Pulsed current at ±2C rates.

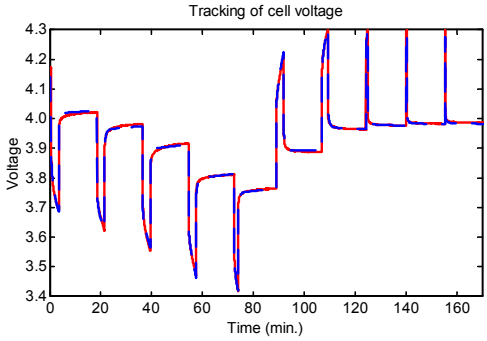

Pulsed current at ±4C rates.

Figure 5: Cell voltage tracking using the enhanced self-correcting model of (12)–(13), (17)–18). Solid red line is true cell voltage; dashed blue line is voltage predicted by cell model. Cell tests were pulsed current at ±1C, ±2C and ±4C rates, punctuated with rest periods.

$$\dot{h}(t) = -\left|\frac{\eta(i(t))i(t)\gamma}{C}\right| h(t) + \left|\frac{\eta(i(t))i(t)\gamma}{C}\right| M(z,\dot{z}). \tag{16}$$

This may be converted into a difference equation for our discrete-time application using standard techniques (assuming that $i(t)$ and $M(z,\dot{z})$ are constant over the sample period):

$$h_{k+1} = \exp\left(-\left|\frac{\eta(i_k)i_k\gamma\Delta t}{C}\right|\right) h_k + \left(1-\exp\left(-\left|\frac{\eta(i_k)i_k\gamma\Delta t}{C}\right|\right)\right) M(z,\dot{z}). \tag{17}$$

Note that this is a linear-time-varying system as the factors multiplying the state and input change with i_k and hence with time. The output equation of the enhanced self-correcting model is changed to be:

$$y_k = \mathrm{OCV}(z_k) + C\left[f_k^I\right] - Ri_k + h_k. \tag{18}$$

4. Cell Testing and Model Fitting Results

In order to compare the abilities of the proposed models to capture a cell's dynamics, we gathered data from some prototype LiPB cells. We used a Tenny thermal chamber set at 25°C and an Arbin cell cycler. In all cases, the cells were fully charged before the tests began. Pulsed discharge cycles punctuated with rest intervals were followed by pulsed charge cycles, again with rest periods. Data points (including voltage, current, Ah discharged, and Ah charged) were collected once per second.

The data was used to identify parameters of the three cell models—one set of parameters was fit for each test. Then, the models were used to predict terminal voltage for the tests. Figures 2–5 show a comparison between model predicted terminal voltage and actual measured terminal voltage for three representative tests: pulsed ±1C rates, pulsed ±2C rates and pulsed ±4C rates. In all plots, the solid red line is the true cell voltage and the dashed blue line is the model's prediction.

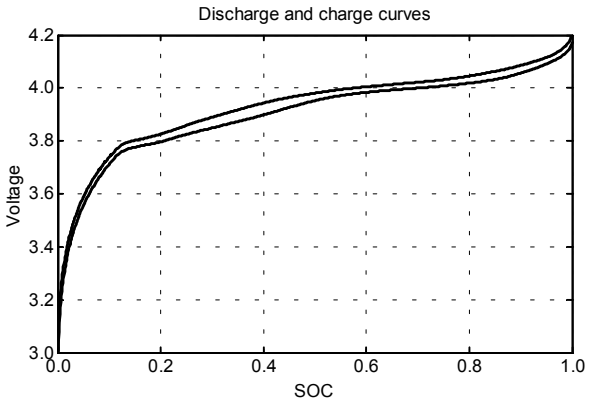

Figure 6: Discharge and charge curves illustrating hysteresis.

Table 1 lists the root-mean-square (RMS) error between the true cell output and the model output. Small RMS errors are desirable. The "combined" model from reference [1] is used as a baseline. We see that the "simple" model of (10) gives very similar performance (about 1% worse, on average) but is easier to implement due to the removal of the log functions and parameters $K_0 \ldots K_4$. The self-correcting model is far better than the "combined" model (about 69% better, on average), and the enhanced self-correcting model better yet (about 18% better than the self-correcting model, on average).

	RMS modeling error (mV) for each cell test		
	±1C Test	±2C Test	±4C Test
Combined model from [1]	19.5	20.2	27.3
Simple model from (10)	20.4	20.8	26.0
Self-correcting model	8.7	6.4	4.8
Enhanced self-correcting model	6.3	5.0	4.6

Table 1: Comparison of four different cell models.

An extended Kalman filter was then run (method from [2]), using the enhanced self-correcting model, to evaluate SOC estimation ability. Figure 7 shows the SOC tracking error, (true SOC minus estimated SOC), where the "true" SOC is computed using the Ah dis/charged reported by the Arbin. The same three representative cell tests are used: pulsed ±1C, ±2C, and ±4C rates. In all plots, solid blue line is the SOC error, and the solid green lines delineate the confidence region of the estimate. Plots are given for the case when the Kalman filter is initialized with the true initial SOC (left column) and when the filter is initialized with an incorrect value (right column). Inset plots in the right column show SOC error and bounds for the first minute to demonstrate convergence of the Kalman estimator. For reference, the true SOC for the ±1C test is plotted in Figure 8.

We see that SOC is very accurately estimated both when the initial SOC state is accurate and when it is not. The error bounds are accurate in both cases. In the case where the initial SOC estimate was incorrect, the Kalman filter converged to within a small neighborhood of the truth in approximately 15 seconds of real time. At some points, the filter wanders slightly away from the true SOC, but then returns due to the self-correcting nature of the model used. Of course, comparable techniques such as Coulomb counting run open-loop, and would never converge to the true value if incorrectly initialized, or if parameters such as cell capacity are not known exactly. Inelegant and problematic *ad hoc* recalibration

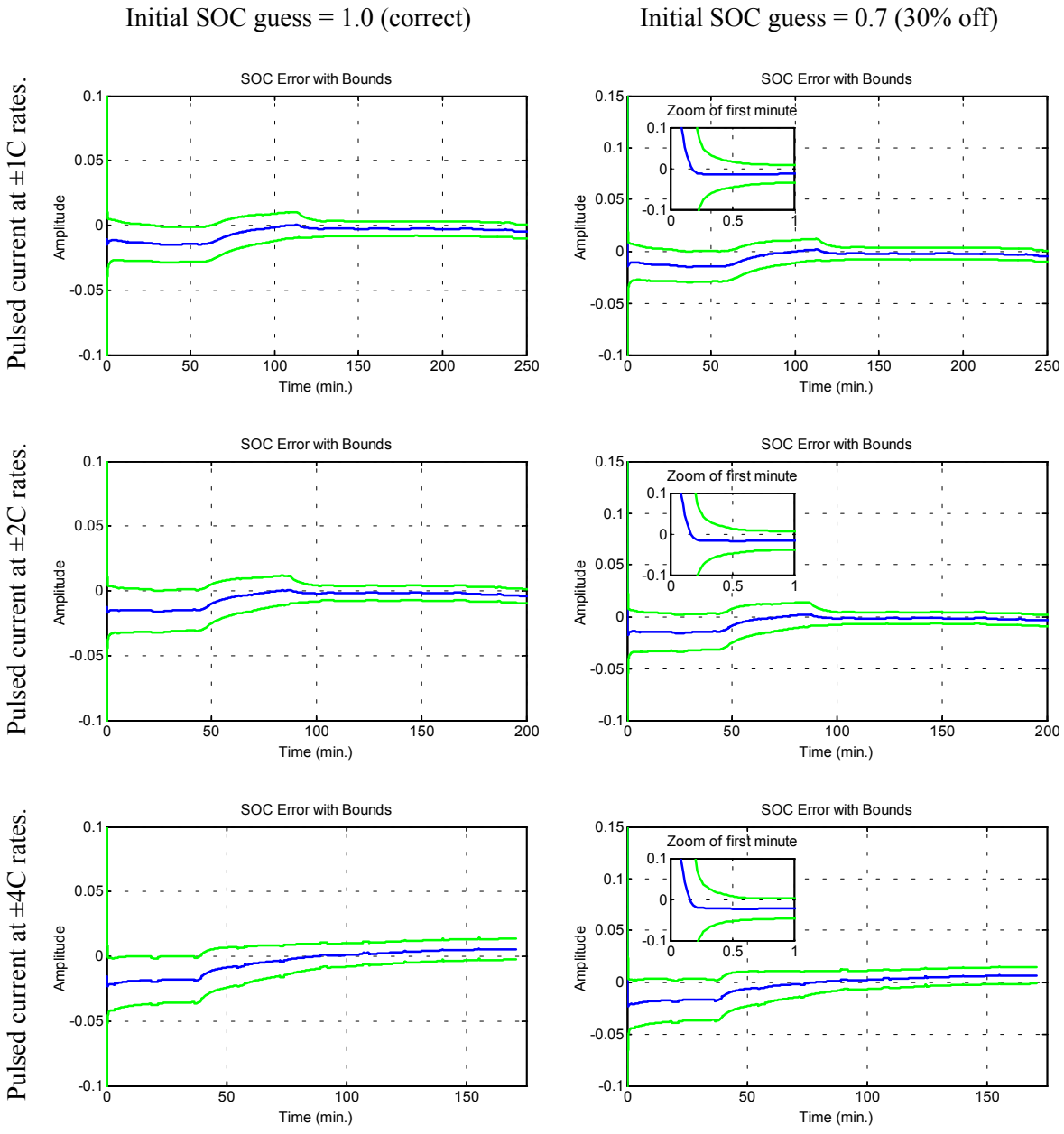

Figure 7: Kalman-filter tracking of SOC—using the enhanced self-correcting model—for correct initial estimate and incorrect initial estimate.

techniques and correction factors are often used to tune the estimate—these are not needed with the Kalman method.

The estimation results obtained here using the enhanced self-correcting model are superior to those experienced using the RBF model in [2], and at a fraction of the complexity. In an embedded implementation, the EKF code that uses the enhanced self-correcting model runs approximately 50 times faster than similar code using the RBF model. The enhanced self-correcting model also has the advantage that its parameters correspond to physical phenomena such as internal resistance, hysteresis and relaxation time constants, so is more readily understood. Furthermore, we have found it to be much more robust.

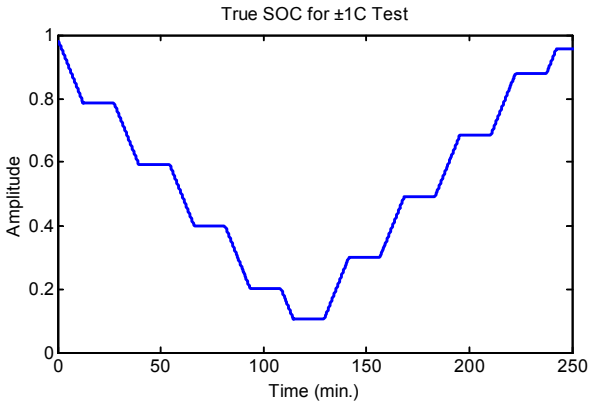

Figure 8: True SOC for ±1C test. The ±2C and ±4C tests are similar.

5. Conclusions

This paper has focused on several mathematical state-space structures for modeling LiPB HEV cell dynamics for the purpose of SOC estimation via Kalman filtering. These models have evolved from those presented in [1–2], and include effects due to: open-circuit voltage, cell relaxation, cell internal resistance, and hysteresis. When used with an extended Kalman filter to estimate SOC, they perform better, are less complex, and are more robust.

6. References

[1] G. Plett, "LiPB Dynamic Cell Models for Kalman-Filter SOC Estimation", in *CD-ROM Proceedings of the 19th Electric Vehicle Symposium* (*EVS19*), Busan Korea, October 2002.

[2] G. Plett, "Kalman-Filter SOC Estimation for LiPB HEV Cells", in *CD-ROM Proceedings of the 19th Electric Vehicle Symposium* (*EVS19*), Busan Korea, October 2002.

[3] S. Piller, M. Perrin and A. Jossen, "Methods for state-of-charge determination and their applications," *Journal of Power Sources*, vol. 96 (2001), pp. 113–120.

[4] V. Srinivasan, J.W. Weidner and J. Newman, "Hysteresis during cycling of nickel hydroxide active material", *Journal of the Electrochemical Society*, vol. 148, no. 9, (2001), pp. A969–980.

7. Affiliation

Dr. Gregory L. Plett, *Assistant Professor,*
Dept. of Electrical and Computer Engineering, University of Colorado at Colorado Springs,
1420 Austin Bluffs Parkway, P.O. Box 7150, Colorado Springs, CO 80933–7150 USA
Tel: +1–719–262–3468, Fax: +1–719–262–3589, E-mail: glp@eas.uccs.edu,
URL: http://mocha-java.uccs.edu, *and consultant to*
Compact Power Inc., 1200 S. Synthes Ave., Monument, CO 80132 USA
Tel: +1–719–488–1600x134, Fax: +1–719–487–9485, E-mail: gplett@compactpower.com.
URL: http://www.compactpower.com/.